Morphology and Fracture Properties of Modified Bisphenol A and Novolac Type Vinyl Ester Resins

J. Karger-Kocsis, O. Gryshchuk

Institute for Composite Materials, Kaiserslautern University of Technology, P.O. Box 3049, D-67653 Kaiserslautern, Germany

Received 2 August 2005; accepted 17 September 2005
DOI 10.1002/app.23220
Published online in Wiley InterScience (www.interscience.wiley.com).

ABSTRACT: The morphology–toughness relationship of vinyl ester resins was studied as a function of their modification. Bisphenol A based and novolac-based vinyl ester resins were modified by a star-shaped polyether polymer with vinyl and hydroxyl functionalities and/or by a polyisocyanate. The polyisocyanate-containing systems were termed vinyl ester/urethane hybrids. The morphology of the crosslinked resins was studied with dynamic mechanical thermal analysis and atomic force microscopy with ion-eroded specimens and discussed. The toughness of the crosslinked resins was assessed by the linear elastic fracture mechanics with compact tension specimens. The fracture toughness and energy changed fairly linearly as functions of M_c and $M_c^{0.5}$, respectively, where M_c is the mean molecular mass between crosslinks. © 2006 Wiley Periodicals, Inc. J Appl Polym Sci 100: 4012–4022, 2006

Key words: atomic force microscopy (AFM); crosslinking; fracture; networks; toughness

INTRODUCTION

Bisphenol A based and novolac-based commercial vinyl ester resins are widely used in various applications. This fact triggers research and development activities, the major target of which is toughness improvement. Vinyl ester resins are produced usually by the reaction of epoxy resins with methacrylic acid[1–5] (cf. Scheme 1). The outcome is a multifunctional resin that, in fact, serves as a crosslinking agent for styrene (and not vice versa), in which the resin is traditionally diluted. Novolac-based vinyl esters (NVEs) have a higher functionality than bisphenol A based vinyl esters (VEs). This is obvious when we compare Schemes 1 and 2. A large body of work deals with the polymerization kinetics, chemorheology, and thermal and mechanical properties of vinyl esters.[6–9] In addition, some studies are also available on the morphology of VE resins.[10–12]

Crosslinked VEs possess good mechanical and excellent thermal properties. The temperature resistance of vinyl esters can be enhanced by the reaction of their hydroxyl groups (see Schemes 1 and 2) with polyisocyanates. The related combinations, called vinyl ester/urethane hybrids (VEUHs), show a glass-transition temperature (T_g) 30–40°C higher than that of the corresponding unmodified, solely styrene-crosslinked resins.[2,11,13–17]

Because of their tight crosslinking, VEs outperform unsaturated polyesters with respect to thermal and solvent resistance. On the other hand, they suffer low toughness similarly to all other thermosets. Toughness-improving strategies follow one or more of the following concepts: (1) the incorporation of fillers and reinforcements, (2) the creation of a rubber dispersion within the VE matrix, and (3) the tailoring of the crosslinked network by the selection of suitable comonomers. More scientific works have dealt with the filling/reinforcement of vinyl esters[18–24] than rubber toughening[25–28] and network modification.[29–32] This is quite surprising as the latter strategies have been extensively adopted for epoxy resins. The major problem with rubber toughening is that the particle size of the functional rubbers can hardly be controlled via phase separation during the very fast copolymerization/crosslinking reaction. To modify the network density, either the type of VE (chemical buildup and molecular mass) or the comonomer (buildup and reactivity) should be varied.[33–36] A recent strategy is to use functional hyperbranched polymers or star-shaped polymers (SSPs) as toughness modifiers, which usually have epoxy and amine functionalities.[37–41] Previous works following this concept for VEs have shown that loosely packed SSPs are for more efficient network modifiers than hyperbranched polymers with a tight structure.[42] SSPs, produced by var-

Correspondence to: J. Karger-Kocsis (karger@ivw.uni-kl.de).
Contract grant sponsor: German Science Foundation; contract grant number: DFG Ka 1202/15.
Contract grant sponsor: Fonds der Chemischen Industrie.

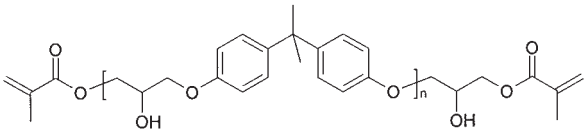

Scheme 1 VE.

ious techniques,[43–46] have already been introduced into polymers as impact and viscosity modifiers.[45,47]

The use of a functional SSP as an impact modifier for VE and VEUH systems had not yet been studied. In this work, an SSP with both vinyl and hydroxyl functionalities (cf. Scheme 3) was used as a modifier for VE, NVE, and the corresponding urethane hybrid resins [VEUH and novolac-based vinyl ester/urethane hybrid (NVEUH)]. The major aims of this analysis were to assess the morphology and clarify its effect on the toughness response of the VE systems.

EXPERIMENTAL

Materials

VE and NVE were styrene-diluted (30 wt %) commercial resins [Daron XP-45-A-2 (VE) and Atlac 590HV (NVE) from DSM Composite Resins, Zwolle, The Netherlands].

For the related urethane hybrids, VEUH and NVEUH, a novolac-based polyisocyanate (NPI; cf. Scheme 4) was introduced at a concentration of 38 phr (i.e., to 100 parts of styrene containing VE, 38 parts of NPI was added). Their curing occurred through the addition of 0.75 parts of dibenzoyl peroxide (Akzo Nobel, Düren, Germany) and 0.15 parts of *N,N*-diethyl aniline accelerator (Akzo Nobel). As a network modifier, an SSP (with vinyl and hydroxyl groups), given in Scheme 3, served. This SSP was composed of a six-arm star poly(propylene oxide-*block*-ethylene oxide) core and a poly(allyl glycidyl ether) shell. The designation 50V18 means 50 vinyl groups and an 18,000 g/mol molecular mass. The synthesis of this SSP was reported earlier.[42] The SSP was incorporated to a concentration of 10 wt % into the corresponding resins.

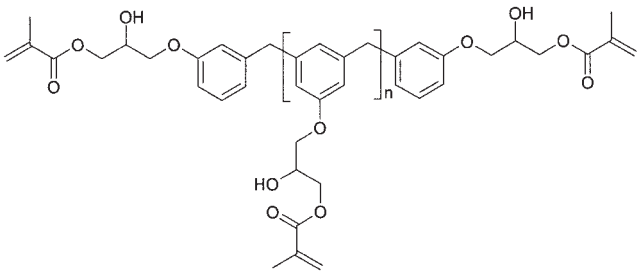

Scheme 2 NVE.

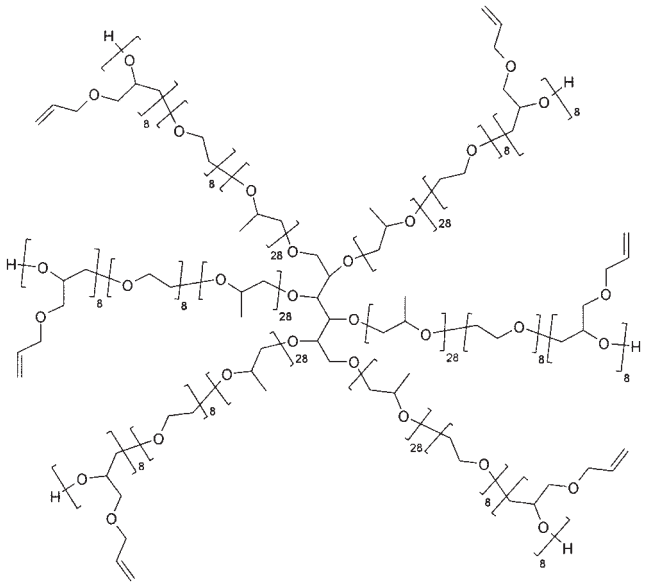

Scheme 3 Structure of the six-arm polyether (SSP) bearing vinyl and hydroxyl groups.

Specimen preparation

Compact tension (CT) specimens (cf. Fig. 1) were produced via the pouring of a homogenized and degassed resin mixture into steel molds. After a mold was filled at room temperature, the following cure sequence was used: 50°C/15 min, 80°C/30 min, 140°C/30 min, and finally 200°C/60 min.

Material characterization

The phase structure of the compositions was characterized by dynamic mechanical thermal analysis (DMTA). DMTA spectra were taken on rectangular specimens in the tensile mode at 10 Hz with an Eplexor 25 N device from Gabo Qualimeter (Ahlden, Germany). The static and cyclic (sinusoidal) loading components were set to 10 N and ±5 N, respectively. DMTA spectra [i.e., the complex modulus (E^*) and mechanical loss factor (tan δ) as functions of temperature T] were measured in the interval of $T = -100$ to final failure at a heating rate of 1°C/min.

The mean molecular mass between crosslinks (M_c) was determined with an equation from rubber elasticity theory:[48–52]

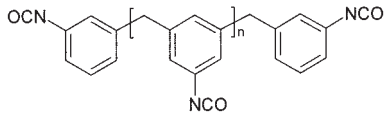

Scheme 4 NPI.

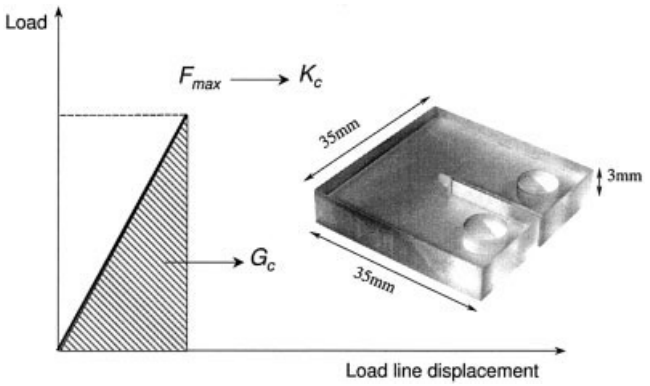

Figure 1 Dimensions of the CT specimen and schematic determination of K_c and G_c.

$$M_c = 3q\frac{\rho RT}{E_r}$$

where q is the front factor (usually 1), ρ is the material density, R is the gas constant, T is the absolute temperature, and E_r is the onset of the modulus in the rubbery region (which was read from the DMTA trace). The onset value, as described in ref. 53, was used as the specimens often broke before the full development of the rubbery plateau.

Information on the morphology of the modified VE, NVE, VEUH, and NVEUH resins was expected from atomic force microscopy (AFM) studies. The polished surface of the specimens was eroded by Ar^+-ion bombardment.[11] This occurred in a secondary neutral mass spectrometer (INA-3, Leybold, Köln, Germany) working at 500 eV of energy. The beam was focused perpendicularly to the polished surface of the specimen. The overall ion dose was 1.9×10^{18} Ar^+/cm^2. The surface profile was scanned by AFM (Veeco/Digital Instruments GmbH, Mannheim, Germany) in the tapping mode, and the related amplitude and height contrast images captured. A commercial silicon cantilever (Pointprobe NCH, Nanosensors, Neuchatel, Switzerland) with a nominal tip radius of less than 10 nm (120-μm cantilever length, 4-μm thickness, 30-μm width, and 42-Nm^{-1} spring constant) was employed under its fundamental resonance frequency of about 330 kHz. The scanning rates were set at 0.5 Hz for all images.

The fracture energy (G_c) and fracture toughness (K_c) were determined on the CT specimens in accordance with the European Structural Integrity Society (ESIS) testing protocol.[54] The CT specimens (cf. Fig. 1) were notched by sawing. Their notch root was sharpened by a razor blade before their tensile loading (mode I) at room temperature on a Zwick 1445 machine (Zwick GmbH, Ulm, Germany) at a crosshead speed of 1 mm/min.

The surfaces of the broken CT specimens were inspected with a scanning electron microscope (JSM-5400, JEOL, Tokyo, Japan). To avoid electric charging, the fracture surface was sputter-coated with an Au/Pd alloy.

RESULTS AND DISCUSSION

In this work, the effects of the resin type (VE and NVE; Schemes 1 and 2), modification by SSP (cf. Scheme 3), and polyisocyanate (cf. Scheme 4) were studied. The polyisocyanate (NPI)-containing resins are denoted VEUH and NVEUH.

Phase structure

Figure 2 depicts E^* (absolute value) and tan δ as a function of temperature for VE, NVE, and their SSP

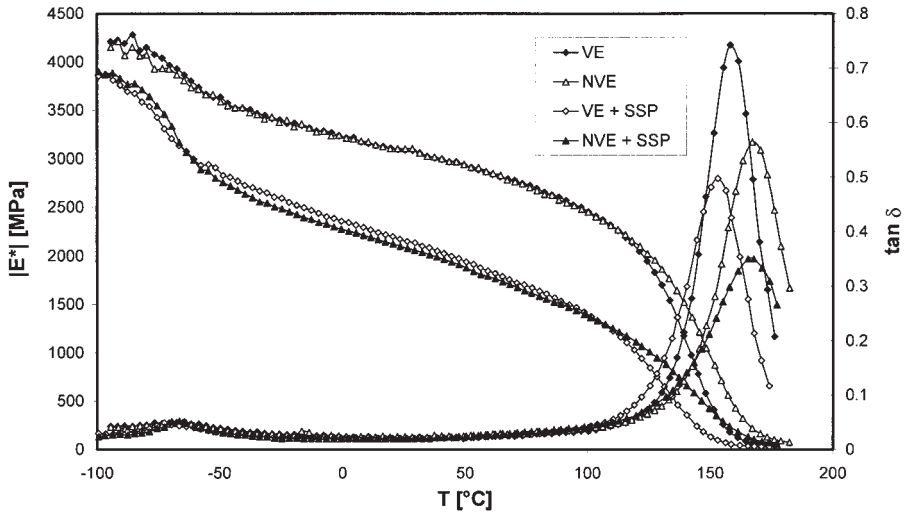

Figure 2 $|E^*|$ and tan δ as functions of the temperature (T) for VE, NVE, and their modifications containing 10 wt % functional SSP.

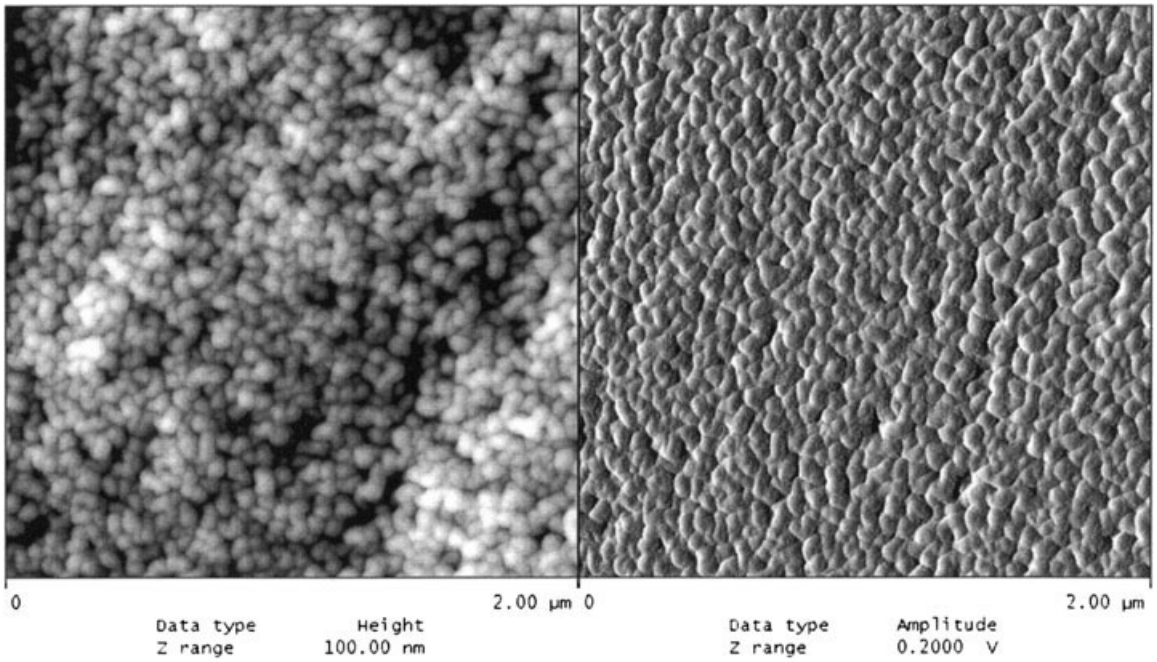

Figure 3 Height (left) and amplitude-modulated (right) AFM images taken from VE.

modifications. The parent VE and NVE resins show two relaxations: the α peak or T_g is at ≈160°C, whereas the β peak is at ≈−65°C. NVE, having a higher functionality and a more rigid structure than VE, exhibits a higher T_g. The reduced molecular mobility of NVE compared with that of VE is also reflected by a reduction in the tan δ peak of the T_g relaxation. The incorporation of functional SSP via free-radical copolymerization reduces the stiffness above the β relaxation and decreases the intensity of tan δ of the T_g relaxation. On the other hand, a small shift (VE), if any (NVE), can be observed with respect with the peak position of T_g. A reduction in T_g is usually due to less tight crosslinking. The stiffness reduction should be linked to a similar change in the apparent network density and/or to the chain flexibility due to the SSP. T_g of the SSP used[42]

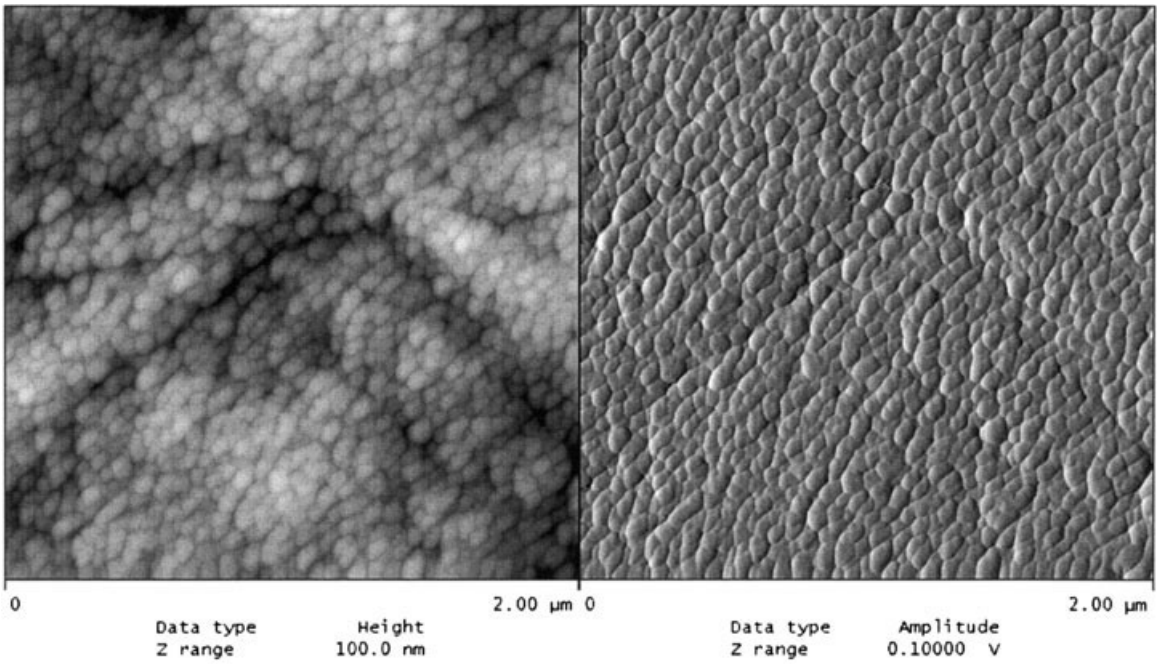

Figure 4 Height (left) and amplitude-modulated (right) AFM images taken from NVE.

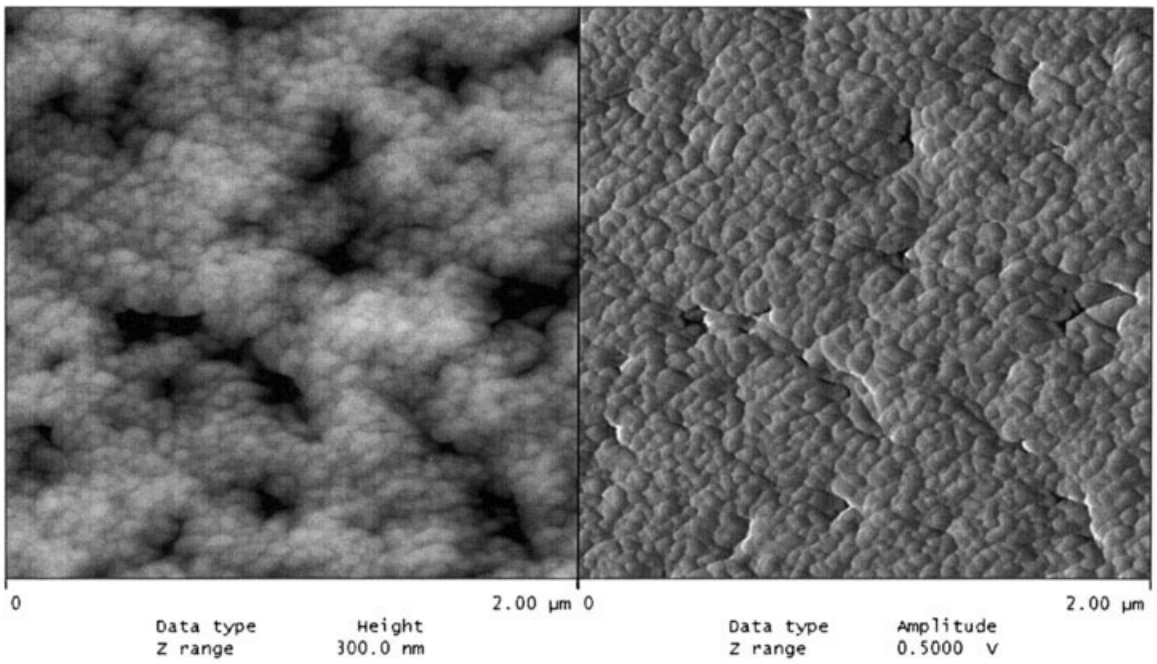

Figure 5 Height (left) and amplitude-modulated (right) AFM images taken from VE modified by 10 wt % SSP.

coincides with that of the β transition of the vinyl esters. The intensity reduction of the T_g transition can be explained by some constraint effects on the molecular/supermolecular level for which the DMTA technique does not deliver any information.

A deeper insight into the morphology was expected from AFM investigations. The related AFM scans are shown in Figures 3–6. VE and NVE exhibit a two-phase structure that is often termed *nodular* and *microgel*. More or less spherical vinyl ester nodules are dispersed in a (poly)styrene and crosslinked vinyl ester matrix. The size of the nodules is in the range of 50–70 nm. The nodules' shape is more regular and their distribution is more homogeneous for NVE (Fig. 4) than for VE (Fig. 3). A similar morphology was disclosed by Mortaigne at al.,[10] who used laser abla-

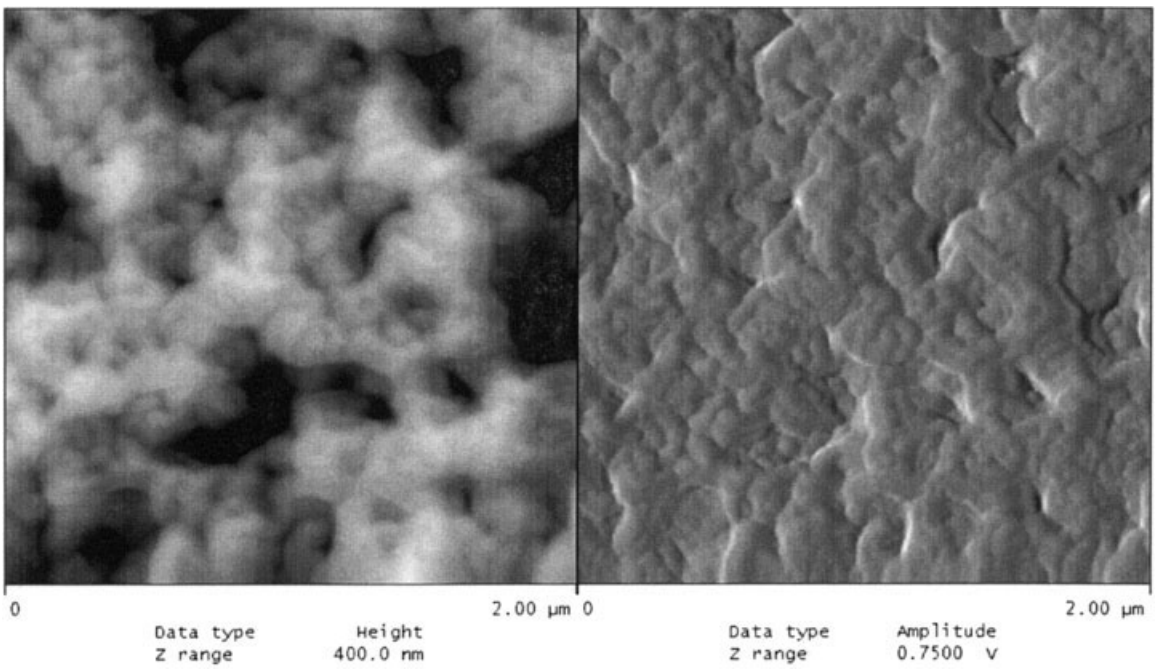

Figure 6 Height (left) and amplitude-modulated (right) AFM images taken from NVE modified by 10 wt % SSP.

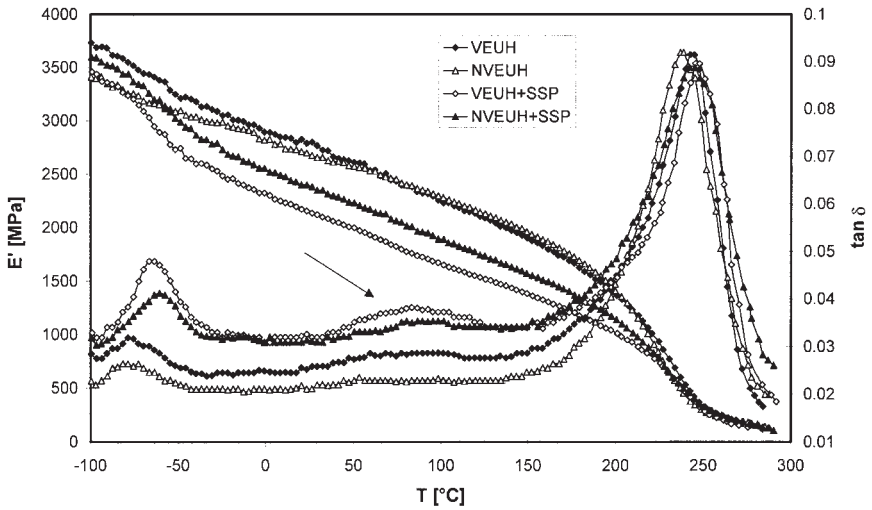

Figure 7 $|E^*|$ and tan δ as functions of temperature (T) for VEUH, NVEUH, and their modifications containing 10 wt % functional SSP.

tion for the physical etching of unsaturated polyester and vinyl ester resins. The nodular structure is still observable for VE plus SSP (Fig. 5). On the other hand, this is less obvious for NVE plus SSP (Fig. 6); this may be a hint of some better compatibility. Comparing the morphologies in Figures 5 and 6, one can claim that SSP mostly affected the matrix formation (see the dark areas, which have lower resistance to ablation) in VE; that is, the nodular structure still remained. On the other hand, SSP influenced the formation of both the nodules (via participation in the crosslinking) and matrix (mostly because of SSP homopolymerization and SPP copolymerization with styrene). The possible homopolymerization and various copolymerization reactions between the components result in various molecular and supermolecular assemblies. Their molecular mobility is different, and this may additionally influence the shrinkage locally. This may be the explanation for the reduced intensity of the α relaxation in the DMTA trace (Fig. 2).

How is the phase structure changing when further crosslinking between the secondary —OH groups of the vinyl esters and/or SSP and —NCO groups of NPI occurs? Figure 7 displays $|E^*|$ and tan δ versus tem-

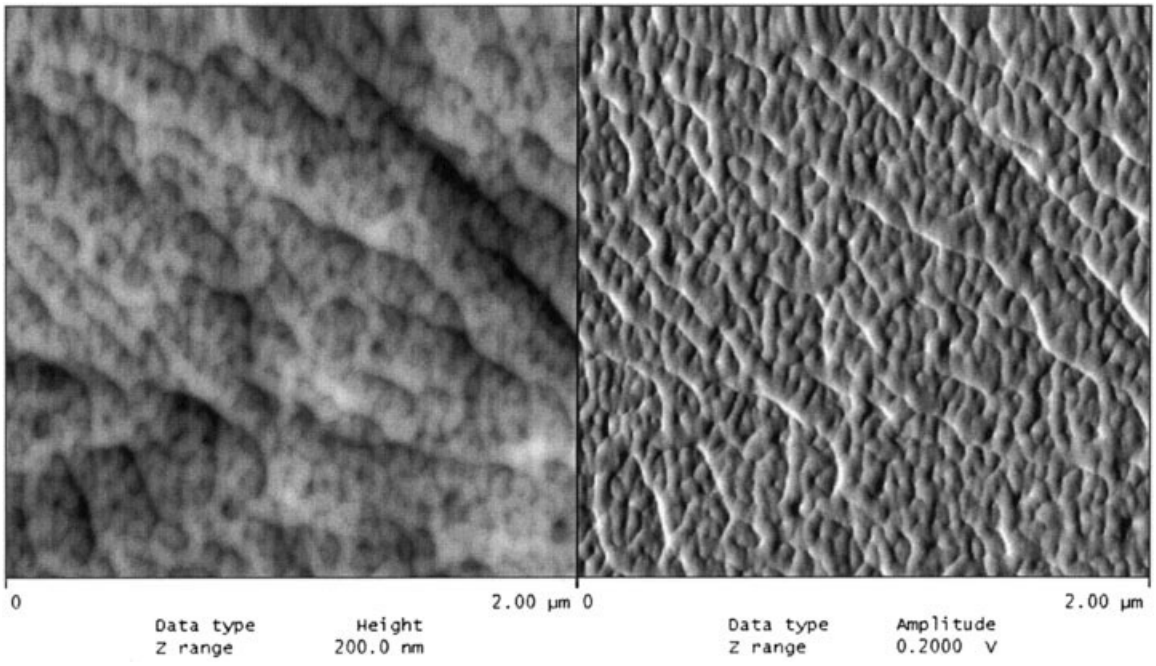

Figure 8 Height (left) and amplitude-modulated (right) AFM images taken from VEUH.

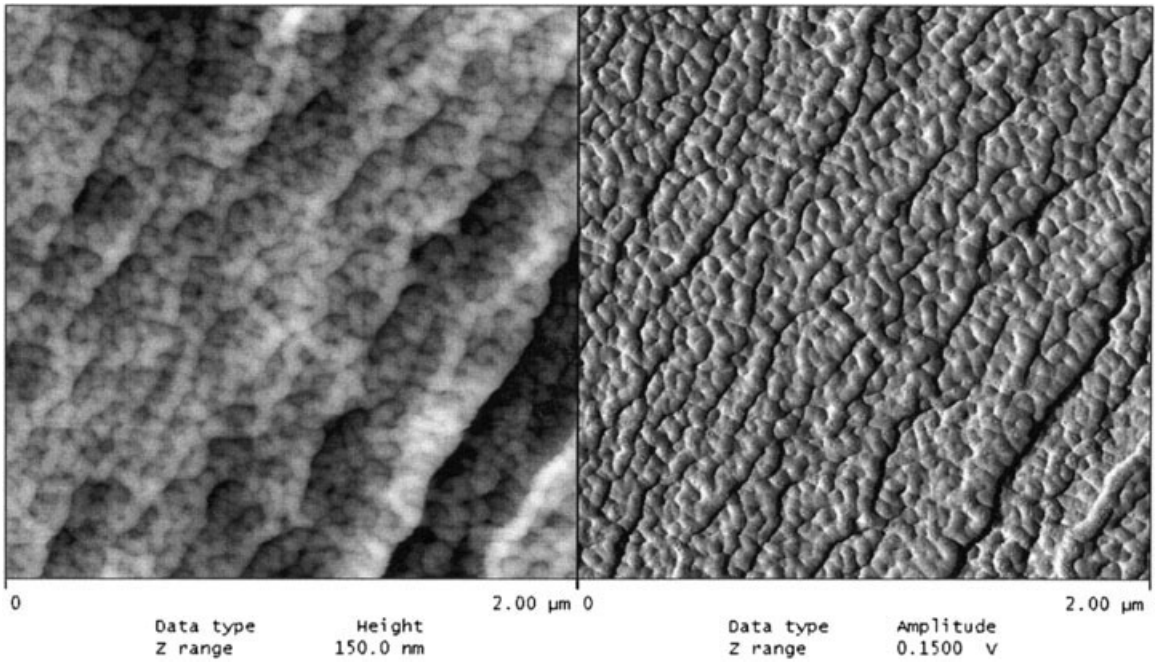

Figure 9 Height (left) and amplitude-modulated (right) AFM images taken from NVEUH.

perature traces for VEUH, NVEUH, and their modifications with 10% SSP. Comparing the DMTA traces in Figures 2 and 7, one can recognize the large improvement in T_g (α relaxation) due to the additional polyurethane-type crosslinking. The onset of a new relaxation peak (≈80°C; marked by arrow) between the α (≈250°C) and β relaxations (≈−70°C) suggests the appearance of an interphase layer. The broad range and low intensity of this peak indicate that this interphase exhibits an inhomogeneous structure. Such an interphase peak often appears in thermosets of interpenetrating network (IPN) structures.[55] The $|E^*|$–temperature traces of VEUH and NVEUH are almost identical. Modification by SSP is accompanied by a stiffness reduction above the β relaxation, without affecting the position of the α peak. Furthermore, the

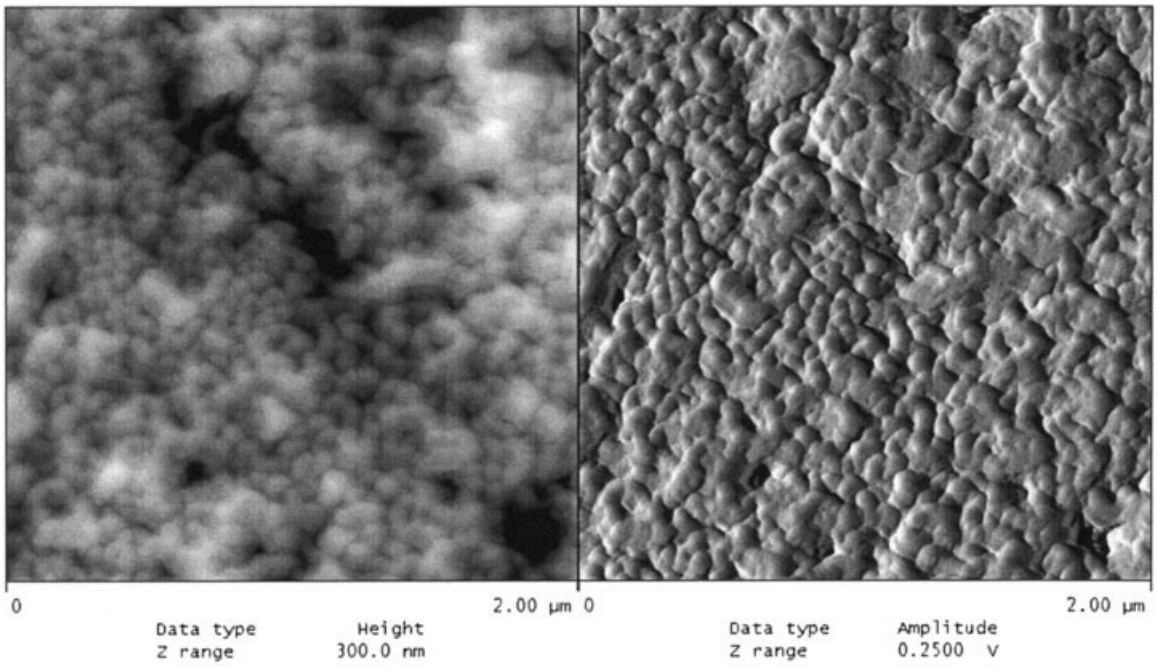

Figure 10 Height (left) and amplitude-modulated (right) AFM images taken from VEUH modified by 10 wt % SSP.

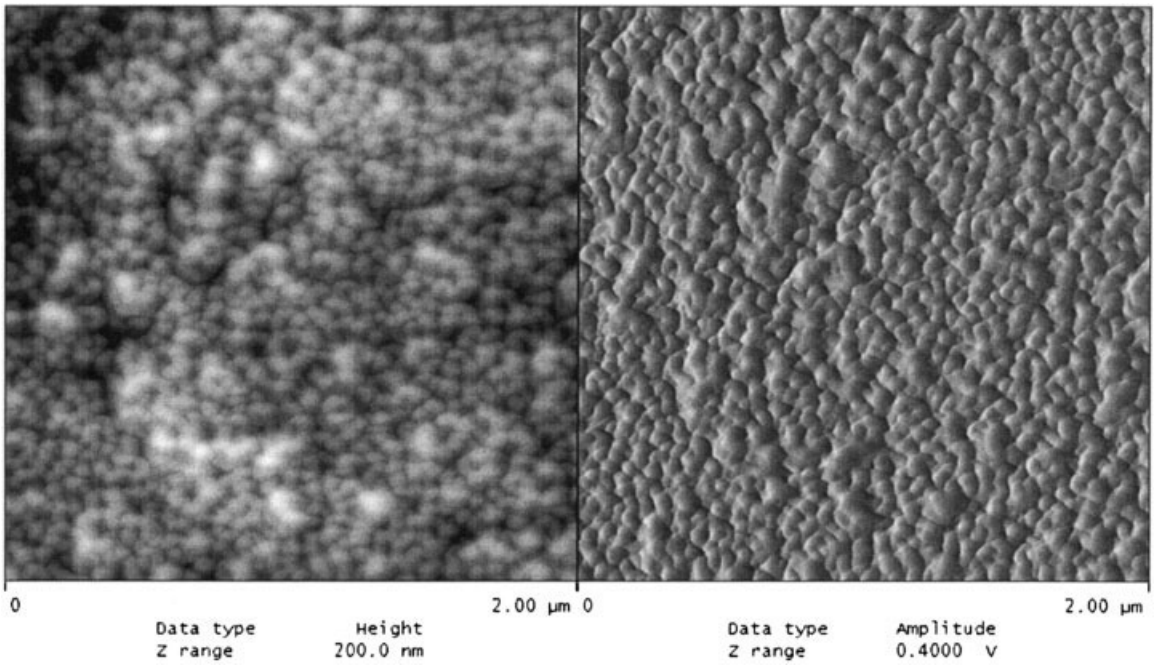

Figure 11 Height (left) and amplitude-modulated (right) AFM images taken from NVEUH modified by 10 wt % SSP.

T_g relaxation of VEUH and NVEUH is much smaller than that of VE and NVE. This suggests a markedly higher crosslinked density and thus lower M_c values for VEUHs.

The morphology of the VEUHs strongly differs from that of the parent vinyl esters (cf. Figs. 8 and 9 with Figs. 3 and 4), and this holds also for SSP-modified versions. Instead of nodules, larger interconnected domains are present in VEUH, which looks like a quasi-IPN structure. Nevertheless, the mean size of the ribbonlike entities agrees with that of the VE nodules. The only difference between VE and VEUH is the onset of an additional crosslinking reaction in the latter resin. The reaction between the secondary —OH of VE and —NCO of NPI should preferentially occur between VE molecules (an intermolecular reaction connecting two nodules) and trigger the formation of a hybrid structure. The morphology of SSP-modified VEUH and NVEUH is shown in Figures 10 and 11. NVEUH plus SSP shows a more homogeneous phase structure than VEUH plus SSP. The structure of the latter system is very heterogeneous. The difference in the size and shape of the particles (nodules) likely represents the outcome of various copolymerization and polyaddition reactions occurring simultaneously and/or consecutively. Nevertheless, modification

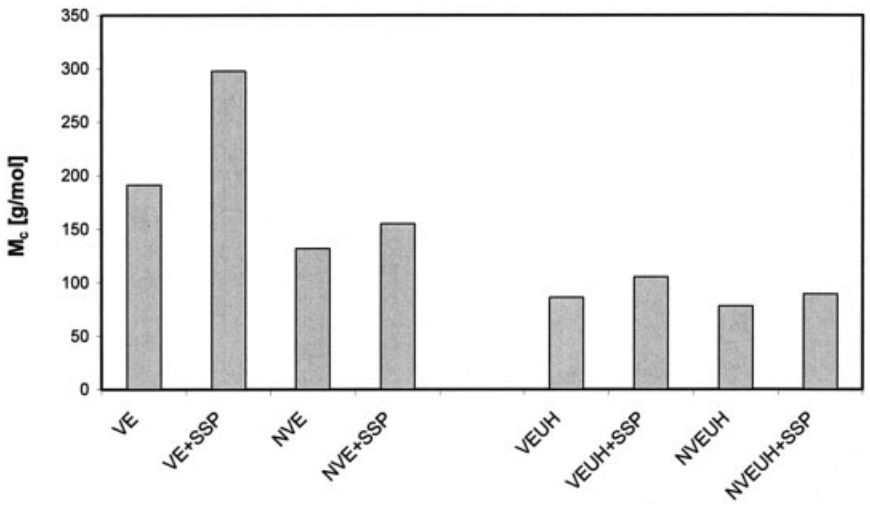

Figure 12 M_c for all compositions.

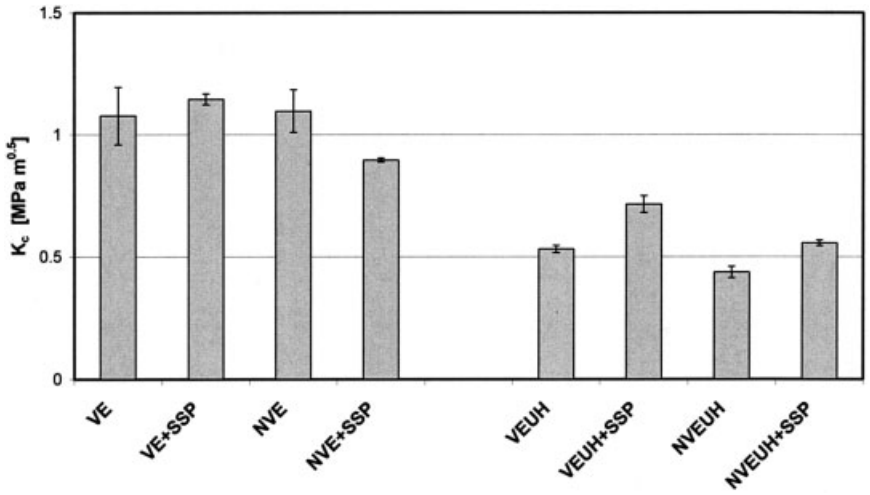

Figure 13 K_c for VE, NVE, VEUH, and NVEUH without and with 10 wt % SSP.

with SSP raises the interphase peak and that of the β relaxation, which is superimposed to that of the T_g value of SSP (cf. Fig. 7).

Apparent crosslinking

A suitable measure of the crosslinking degree is M_c, which is inversely proportional to the crosslink density. Figure 12 depicts the M_c values for the vinyl ester and vinyl ester/urethane systems studied. M_c decreases with increasing vinyl functionality (VE and NVE) and additional crosslinking via the polyurethane route (VEUH and NVEUH). On the other hand, modification with SSP increases M_c, and this increment depends on the type of base resin.

Fracture mechanical data and their network dependence

K_c and G_c values for the studied resin combinations are displayed in Figures 13 and 14, respectively. The K_c and G_c values are practically the same for VE and NVE. Their modifications with SSP are less efficient tools to improve the fracture mechanical response. A small G_c improvement was noticed for the VE system (Fig. 14). On the other hand, the modification of VEUHs with a functional SSP is a good strategy, especially when G_c should be improved. K_c and G_c (cf. Figs. 13 and 14) do not rise for NVE when it is modified with SSP, which is accompanied by an increase in M_c (cf. Fig. 12). The authors have no explanation for this unexpected behavior.

Because thermosets fail mostly by shear deformation and the latter depends on the crosslink density, correlations between fracture mechanical and network parameters should exist. G_c linearly changes with $M_c^{0.5}$ for many thermosets that have, however, a homogeneous network structure.[56–59] This relationship is based on the rubber elasticity theory.[48] A linear relationship between G_c and $M_c^{0.5}$ means that at the same time a similar tendency should hold between K_c

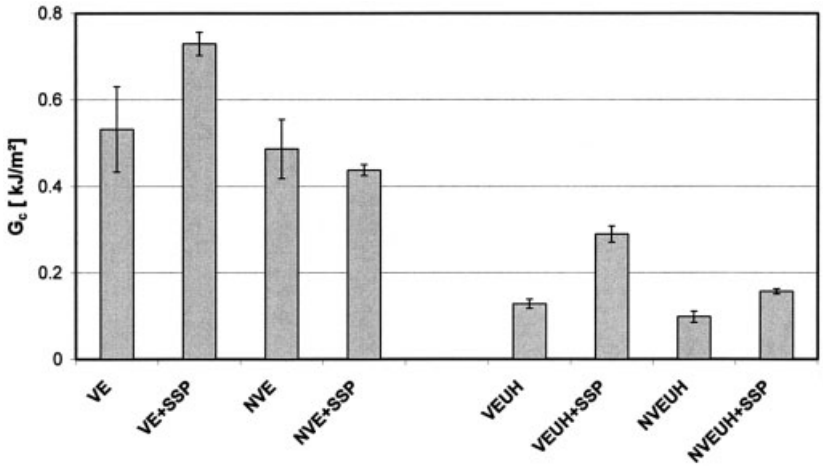

Figure 14 G_c for VE, NVE, VEUH, and NVEUH without and with 10 wt % SSP.

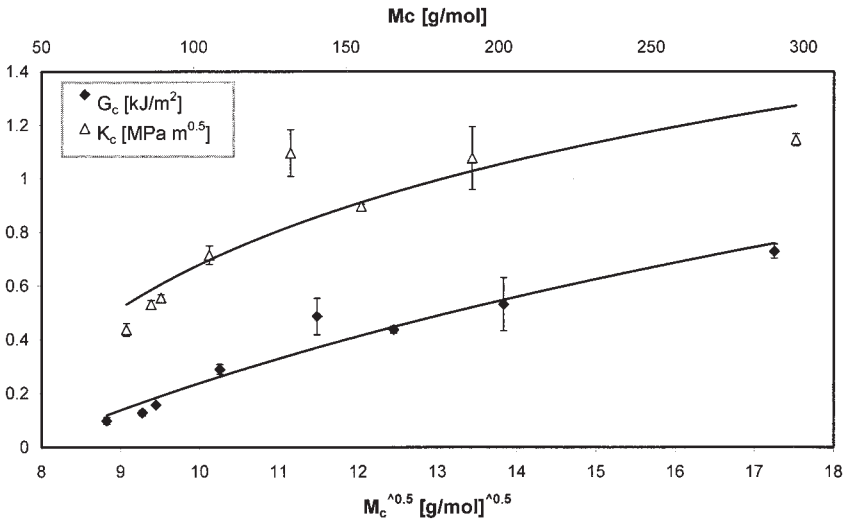

Figure 15 K_c as a function of M_c and G_c as a function of $M_c^{0.5}$.

and M_c. The results in Figure 15 seem to corroborate these predictions. It has to be emphasized that the ambiguity with the M_c determination (associated with a scatter along the abscissa) is disregarded and would mostly affect the K_c–M_c relationship. The results in Figure 15 are not very surprising as in the past the aforementioned relationships have been found valid for thermosets of very heterogeneous structures, as well.

CONCLUSIONS

On the basis of this work devoted to studying the morphology-related fracture behavior of various vinyl ester resins (VE and NVE) modified by vinyl/hydroxyl functional SSP and/or polyisocyanate (VEUH and NVEUH), the following conclusions can be drawn:

- Ar^+ bombardment is a suitable sample preparation technique for studying the morphology of these thermosets via AFM.
- The nodular morphology of the vinyl ester resins changed as a function of the type and modification. The nodular structure of NVE was more compact than that of VE. Their modification by SSP resulted in a more heterogeneous phase structure, which was likely affected by the compatibility between SSP and vinyl ester. Additional crosslinking via polyurethane chemistry (i.e., by the addition of NPI) altered the initial gel structure as the nodules became locally agglomerated. The modification of VEUH and NVEUH by SSP resulted in a nodular phase structure.
- The incorporation of SSP was accompanied by a stiffness decrease above the β relaxation of vinyl ester (which was superimposed to the T_g value of SSP). However, T_g (α relaxation) of the resins was less affected. Adding polyisocyanate (NPI) improved markedly the T_g values of the resins.
- K_c and G_c showed a fairly linear relation as a function of M_c and the square root of M_c, respectively. This supports the idea that the theory of rubber elasticity may be used even for heterogeneous systems such as the studied systems.

The authors are indebted to Mülhaupt (Freiburg) and Schmitt (Kaiserslautern) for supplying the star-shaped polymer and performing the atomic force microscopy tests, respectively.

References

1. Burchill, P. J.; Pearce, P. J. In Polymeric Materials Encyclopedia; Salomone, J. C., Ed.; CRC: Boca Raton, FL, 1996; Vol. 3, p 2204.
2. Gawdzik, B.; Matynia, T. J Appl Polym Sci 2001, 81, 2062.
3. Agrawal, S.; Singhal, R.; Rai, J. S. P. J Macromol Sci Pure Appl Chem 1999, 36, 741.
4. Cook, W. D.; Simon, G. P.; Burchill, P. J. J Appl Polym Sci 1997, 64, 769.
5. Abadie, M. J. M.; Mekhissi, K.; Burchill, P. J. J Appl Polym Sci 2002, 84, 1146.
6. Brill, R. P.; Palmese, G. R. J Appl Polym Sci 2000, 76, 1572.
7. Ziaee, S.; Palmese, G. R. J Appl Polym Sci 1999, 37, 725.
8. Gaur, B.; Rai, J. S. P. Eur Polym J 1993, 29, 1149.
9. Dhulipala, R.; Kreig, G.; Hawley, M. C. Polym Mater Sci Eng 1993, 68, 175.
10. Mortaigne, B.; Feltz, B.; Laurens, P. J Appl Polym Sci 1997, 66, 1703.
11. Karger-Kocsis, J.; Gryshchuk, O.; Schmitt, S. J Mater Sci 2003, 38, 413.
12. Rey, L.; Duchet, J.; Galy, J.; Sautereau, H.; Vouagner, D.; Carrion, L. Polymer 2002, 43, 4375.
13. Pachha, R. R.; Thakkar, J. R.; Patel, R. D. High Perform Polym 1993, 5, 207.
14. Pachha, R. R.; Thakkar, J. R.; Patel, R. D.; Patel, R. G. Angew Makromol Chem 1994, 214, 211.
15. Jost, N.; Karger-Kocsis, J. Polymer 2002, 43, 1383.

16. Verleg, R. L.; Bargsma, A.; Koning, A. D. Proceedings of the 28th International AVK Conference on Composites Today and Tomorrow, Baden-Baden, Germany, 1997; p 1.
17. Verleg, R. L. Proceedings of the BPF Composite Conference, Zwolle, The Netherlands, 1996; p 35.
18. Burchill, P. J.; Kootsookos, A.; Lau, M. J Mater Sci 2001, 36, 4239.
19. Verghese, K. N. E.; Jensen, R. E.; Lesko, J. J.; Ward, T. C. Polymer 2001, 42, 1633.
20. Roy, R.; Sarkar, B. K.; Rana, A. K.; Bose, N. R. Bull Mater Sci Part 1 2001, 24, 79.
21. Compston, P.; Jar, P.-Y. B.; Burchill, P. J.; Takahashi, K. In Fracture of Polymers, Composites and Adhesives; Williams, J. G.; Pavan, A., Eds.; Elsevier: Oxford, 2000; p 37.
22. Nazareth da Silva, A. L.; Teixeira, S. C.; Widal, A. C.; Coutinho, F. M. Polym Test 2001, 20, 895.
23. Sagi-Mana, D.; Narkis, M.; Siegmann, A. J Appl Polym Sci 1998, 69, 2229.
24. Ray, D.; Sarkar, B. K.; Bose, N. R. Compos A 2002, 33, 233.
25. Dreerman, E.; Narkis, M.; Siegmann, A. J Appl Polym Sci 1999, 72, 647.
26. Auad, M. L.; Frontini, P. M.; Borrajo, J.; Aranguren, M. I. Polymer 2001, 42, 3723.
27. Lee, F. S. M. International Encyclopedia of Composites; VCH: New York, 1991; p 489.
28. Pham, S.; Burchill, P. J. Polymer 1995, 36, 3279.
29. Bellenger, V.; Verdu, J.; Ganem, M.; Mortaigne, B. Polym Compos 1994, 2, 9.
30. Li, H.; Burts, E.; Bears, K. J Compos Mater 2000, 34, 1521.
31. Shan, L.; Robertson, C. G.; Verghese, K. N. E. J Appl Polym Sci 2001, 80, 917.
32. Li, H.; Rosario, A. C.; Davis, S. V. J Adv Mater 1997, 28, 55.
33. Padma, G.; Varma, I. K.; Sinha, T. J. M.; Patel, D. M. Angew Makromol Chem 1993, 211, 157.
34. Malik, M.; Choudhary, V.; Varma, I. K. J Appl Polym Sci 2001, 82, 416.
35. Choudhary, M. S.; Varma, I. K. Angew Makromol Chem 1993, 209, 33.
36. Bellenger, V.; Verdu, J.; Ganem, M.; Mortaigne, B. Polym Compos 1994, 2, 17.
37. Mezzenga, R.; Pettersson, B.; Månson, J.-A. E. Polym Bull 2001, 46, 419.
38. Mezzenga, R.; Boogh, L.; Månson, J. A. Compos Sci Technol 2001, 5, 787.
39. Mezzenga, R.; Plummer, C. J.; Boogh, L.; Månson, J. A. Polymer 2001, 42, 305.
40. Eom, Y.; Boogh, L.; Michaud, V.; Månson, J.-A. Polym Compos 2002, 23, 1044.
41. Gryshchuk, O.; Jost, N.; Karger-Kocsis, J. Polymer 2002, 43, 4763.
42. Karger-Kocsis, J.; Gryshchuk, O.; Fröhlich, J.; Kautz, H.; Frey, H.; Mülhaupt, R. Polymer 2004, 45, 1185.
43. Mishra, M. K.; Kobayashi, S. Star and Hyperbranched Polymers; Marcel Dekker: New York, 1999.
44. Simms, J. A. Rubber Chem Technol 1991, 64, 139.
45. Vamvakaki, M.; Hadjiyannakou, S. C.; Loizidou, E.; Patrickios, C. S.; Armes, S. P.; Billingham, N. C. Chem Mater 2001, 13, 4738.
46. Vamvakaki, M.; Patrickios, C. S. Chem Mater 2002, 14, 1630.
47. Simms, J. A.; Spinelli, H. J. J Coat Technol 1987, 59, 125.
48. Ferry, J. D. Viscoelastic Properties of Polymers; Wiley: New York, 1980.
49. Levita, G.; De Petris, S.; Marchetti, A.; Lazzeri, A. J Mater Sci 1991, 26, 2325.
50. Varley, R. J.; Hodgkin, J. H.; Simon, G. P. J Appl Polym Sci 2000, 77, 237.
51. Un, B. K.; Young, J. J.; Kim, J.; Lee, S.-S.; Park, M.; Lim, S. J Appl Polym Sci 2001, 79, 38.
52. Crawford, E.; Lesser, A. J. J Polym Sci Part B: Polym Phys 1998, 36, 1371.
53. Karger-Kocsis, J.; Gremmels, J. J Appl Polym Sci 2001, 78, 1139.
54. Williams, J. G. In Fracture Mechanics Testing Methods for Polymer Adhesives and Composites; Moore, D. R.; Pavan, A.; Williams, J. G., Eds.; ESIS Publication 28; Elsevier: Oxford, 2001; p 11
55. Lipatov, Y. S. Pure Appl Chem 1985, 57, 1691.
56. Kang, B. U.; Jho, J. Y.; Kim, J.; Lee, S. S.; Park, M.; Lim, S.; Choe, C. R. J Appl Polym Sci 2001, 79, 38.
57. Flipsen, T. A. C.; Derks, R.; Van Der Vegt, H.; Stenekes, R.; Pennings, A. J.; Hadziioannou, G. J Polym Sci Part B: Polym Phys 1997, 35, 1311.
58. Kaiser, T. Prog Polym Sci 1989, 14, 373.
59. Gupta, V. B.; Drzal, L. T.; Lee, C. Y.-C.; Rich, M. J. Polym Eng Sci 1985, 25, 812.